Order-α_s calculation of hadronic ZZ production

J. Ohnemus and J. F. Owens
Department of Physics, Florida State University, Tallahassee, Florida 32306
(Received 17 December 1990; revised manuscript received 21 February 1991)

An order-α_s calculation of $p\overset{(-)}{p} \to ZZ + X$ is presented. Results are given for the total cross section and differential distributions for Fermilab Tevatron, CERN Large Hadron Collider, and Superconducting Super Collider energies. The calculation utilizes a combination of analytic and Monte Carlo integration methods which makes it easy to calculate a variety of observables and to impose experimental cuts.

I. INTRODUCTION

Pair production of Z bosons at hadron supercolliders is an important background to heavy-Higgs-boson production. If the Higgs boson is heavier than twice the Z-boson mass, it will decay almost exclusively into W- or Z-boson pairs.[1] The existence of the Higgs boson would then be signaled by a peak in the invariant-mass distribution of the weak-boson pair. It is therefore important to precisely calculate the continuum production of vector-boson pairs in order to get a realistic estimate of the signal-to-background ratio.

The main background to detecting a heavy Higgs boson in the ZZ decay mode at hadron colliders is the continuum production of Z-boson pairs. The major source of continuum Z pairs is $q\bar{q}$ annihilation.[2] Two other sources are gluon fusion[3,4] and weak-boson fusion.[5] The gluon-fusion production rate is 60–70 % as large as the lowest-order $q\bar{q}$ rate.[4] In weak-boson fusion the incoming quarks radiate two vector bosons which subsequently scatter off each other. This process is mainly of interest as a source of Higgs bosons, with the Higgs boson appearing as an s-channel resonance. Away from the Higgs-boson peak, the weak-boson fusion production rate is only a small fraction of the basic $q\bar{q} \to ZZ$ production rate. Pair production of Z bosons in association with jets has also been calculated.[6]

Until now ZZ production has been calculated only in the leading-logarithm approximation and the order-α_s corrections to ZZ production have only been estimated[7] using the soft-gluon approximation.[8] In this paper we present a complete next-to-leading-logarithm (NLL) calculation of hadronic ZZ production. At the parton level this involves computing the contributions from the $2 \to 3$ real emission processes $q\bar{q} \to ZZg$, $qg \to ZZq$, and $\bar{q}g \to ZZ\bar{q}$ as well as the one-loop corrections to the $2 \to 2$ process $q\bar{q} \to ZZ$. The focus of the present calculation is on the order-α_s corrections to ZZ production. Accordingly, the order-α_s^2 gluon-fusion contribution has not been included. However, this contribution should eventually be included when calculating the full ZZ continuum background since it can be significant at the energy of the Superconducting Super Collider (SSC).

The NLL calculation presented here makes use of a combination of analytic and Monte Carlo integration methods. Similar methods have been used to perform NLL calculations for direct photon production,[9] photoproduction,[10] symmetric di-hadron production,[11] and W production.[12] The Monte Carlo approach to NLL calculations has many advantages over a purely analytic calculation. The Monte Carlo approach allows one to calculate any number of observables simultaneously by simply histogramming the appropriate quantities. Furthermore, it is easy to tailor the Monte Carlo calculation to different experimental conditions, for example, detector acceptances, experimental cuts, and jet definitions. Also, with the Monte Carlo approach one can study the dependence of the cross section on the choice of scale, the size of the NLL corrections for different observables, and the variation of the NLL corrections in different regions of phase space.

The remainder of this paper is organized as follows. Section II describes the techniques used in the Monte Carlo approach to NLL calculations. The NLL calculation of ZZ production is described in Sec. III. Results are presented in Sec. IV and summary remarks are given in Sec. V. Finally, there are four appendixes containing details of the regularization of γ_5 and lengthy expressions from the calculation.

II. MONTE CARLO FORMALISM

The Monte Carlo formalism for NLL calculations has been described in detail in Refs. 9–11 so the discussion here will be brief. The basic challenge is to design a program which retains the versatility inherent in a Monte Carlo approach while ensuring that all of the required cancellations of singularities still take place. In order to discuss the technique for isolating the various singularities, let the four-vectors of the two-body and three-body subprocesses be labeled by $p_1 + p_2 \to p_3 + p_4$ and $p_1+p_2 \to p_3+p_4+p_5$, respectively, and define the Lorentz scalars $s_{ij} = (p_i+p_j)^2$ and $t_{ij} = (p_i-p_j)^2$. First, any ultraviolet (UV) singularities associated with the one-loop

contributions are regulated using the method of dimensional regularization[13] and subtracted using the modified minimal-subtraction ($\overline{\rm MS}$) scheme.[14] Similarly, dimensional regularization is used to treat the infrared (IR), soft, and collinear divergences. As noted in Sec. III B, there are no UV singularities in the current calculation. Next, we introduce soft and collinear cutoff parameters δ_s and δ_c whose purpose is to allow the separation of phase space into singular and finite regions. For the three-body subprocesses, the soft singularities are associated with the phase-space region where a final-state gluon becomes soft. The soft region is defined to be the region where the gluon energy in the subprocess rest frame becomes less than $\delta_s\sqrt{s}_{12}/2$. If δ_s is chosen to be sufficiently small, then the relevant three-body subprocesses can be evaluated using the soft-gluon approximation. The resulting expression is then easily integrated over the soft region of phase space. At this stage, the integrated soft piece is a two-body contribution and the soft and infrared singularities cancel explicitly. Next, the collinear regions of phase space are defined to be those regions where any invariant (s_{ij} or t_{ij}) becomes smaller in magnitude than $\delta_c\, s_{12}$. If δ_c is chosen to be sufficiently small, then in each collinear region the relevant subprocess can be evaluated using the leading-pole approximation. The result is easily integrated in N dimensions, thereby explicitly displaying the collinear singularities which are then factorized and included in the relevant structure functions. At this point, the remainder of three-body phase space contains no singularities and the subprocesses can be evaluated in four dimensions.

The calculation now consists of two pieces—a set of two-body contributions and a set of three-body contributions. Each set consists of finite parts, all singularities having been canceled, subtracted, or factorized. At this stage both pieces depend on the values chosen for the two theoretical cutoffs δ_s and δ_c so that each piece by itself has no intrinsic meaning. However, when the two- and three-body contributions are combined to form a suitably inclusive observable, all dependence on the cutoffs cancels. It turns out that the answers are stable against variations of these cutoffs over quite a wide range, which is as it should be. The cutoffs merely serve to distinguish the regions where the phase-space integrations are done by hand from those where they are done by Monte Carlo integration. When the results are added together, the precise location of the boundary between the two regions is not relevant. The results reported below are stable to reasonable variations in the cutoffs, thus providing a check on the calculation.

III. NEXT-TO-LEADING-LOGARITHM FORMALISM

A. Born process

The two Feynman diagrams which contribute to the Born amplitude for the reaction

$$q(p_1)+\bar{q}(p_2)\longrightarrow Z(p_3)+Z(p_4) \tag{1}$$

are shown in Fig. 1. The Born amplitude in N dimensions is

$$\mathcal{M}^{\rm Born}=\delta_{i_1 i_2}\,e^2\,\mu^{4-N}\sum_{\tau=\pm}\left(g_\tau^{qZq}\right)^2\epsilon_\mu^*(p_3)\,\epsilon_\nu^*(p_4)\bar{V}(p_2)P_{-\tau}\left(\gamma^\nu\frac{\not p_1-\not p_3}{(p_1-p_3)^2}\gamma^\mu+\gamma^\mu\frac{\not p_1-\not p_4}{(p_1-p_4)^2}\gamma^\nu\right)U(p_1)\,, \tag{2}$$

where $\delta_{i_1 i_2}$ is the color tensor (i_1, and i_2 are color indices for quarks 1 and 2), e is the electromagnetic coupling constant, μ is a mass parameter introduced to keep the couplings dimensionless, $\epsilon_\mu^*(p_3)$ and $\epsilon_\nu^*(p_4)$ are the Z-boson polarization tensors, and P_τ denotes the left-right projection operator $P_\tau=\frac{1}{2}(1+\tau\gamma_5)$. The right- and left-handed Z-boson–to–fermion couplings are denoted by $g_\pm^{qZq}$:

$$g_+^{fZf}=-Q_f\tan\theta_W\,,\quad g_-^{fZf}=\frac{T_3^f}{\sin\theta_W\cos\theta_W}-Q_f\tan\theta_W\,, \tag{3}$$

where Q_f and T_3^f denote the electric charge (in units of the proton charge e) and the third component of weak isospin of the fermion f, and θ_W is the weak mixing angle.

The squared amplitude summed over final-state polarizations and initial-state spins is

$$\begin{aligned}|\mathcal{M}^{\rm Born}|^2=\;&N_C e^4(\mu^2)^{4-N}[(g_-^{qZq})^4+(g_+^{qZq})^4](N-2)\\&\times\left\{(N-2)\left[\frac{t}{u}+\frac{u}{t}-M_Z^4\left(\frac{1}{t^2}+\frac{1}{u^2}\right)\right]+8\frac{M_Z^2 s}{tu}+2(N-4)\left(1-\frac{M_Z^4}{tu}\right)\right\}\,,\end{aligned} \tag{4}$$

where N_C is the number of colors and the kinematic invariants are defined by

$$s=(p_1+p_2)^2\,,\quad t=(p_1-p_3)^2\,,\quad u=(p_1-p_4)^2\,. \tag{5}$$

The details for treating γ_5 in N dimensions are described in Appendix A. The algebra for this paper was evaluated using the algebraic manipulation program FORM.[15] Setting $N=4-2\epsilon$, the squared amplitude becomes

$$|\mathcal{M}^{\rm Born}|^2 = 4N_C e^4 \mu^{4\epsilon}[(g_-^{qZq})^4 + (g_+^{qZq})^4]$$
$$\times\left\{\left[\frac{t}{u}+\frac{u}{t}-M_Z^4\left(\frac{1}{t^2}+\frac{1}{u^2}\right)+4\frac{M_Z^2 s}{tu}\right]-\epsilon\left[\frac{t}{u}+\frac{u}{t}-2M_Z^4\left(\frac{1}{t^2}+\frac{1}{u^2}\right)+\frac{1}{tu}(2M_Z^4+s^2)\right]\right.$$
$$\left.+\epsilon^2\left[\frac{t}{u}+\frac{u}{t}-M_Z^4\left(\frac{1}{t^2}+\frac{1}{u^2}\right)+2\left(1-\frac{M_Z^4}{tu}\right)\right]\right\}, \tag{6}$$

which for later convenience we write as

$$|\mathcal{M}^{\rm Born}|^2 = |\mathcal{M}_0^{\rm Born}|^2 + \epsilon|\mathcal{M}_1^{\rm Born}|^2 + \epsilon^2|\mathcal{M}_2^{\rm Born}|^2 . \tag{7}$$

The Born subprocess cross section is

$$d\hat{\sigma}^{\rm Born}(q\bar{q}\to ZZ) = \frac{1}{4}\frac{1}{9}\frac{1}{2}\frac{1}{2s}|\mathcal{M}^{\rm Born}|^2 d^N\Phi_2 , \tag{8}$$

where the factors $\frac{1}{4}$, $\frac{1}{9}$, and $\frac{1}{2}$ are the spin-average, color-average, and identical-particle factors, respectively, and the two-body phase space is

$$d^N\Phi_2 = \frac{1}{8\pi}\left(\frac{4\pi}{s}\right)^{\epsilon}\frac{1}{\Gamma(1-\epsilon)}\left(1-\frac{4M_Z^2}{s}\right)^{1/2-\epsilon} v^{-\epsilon}(1-v)^{-\epsilon}\,dv , \tag{9}$$

with $v = \frac{1}{2}(1+\cos\theta)$. Decomposing $|\mathcal{M}^{\rm Born}|^2$ as in Eq. (7), the Born cross section can be written

$$d\hat{\sigma}^{\rm Born} = d\hat{\sigma}_0^{\rm Born} + \epsilon\, d\hat{\sigma}_1^{\rm Born} + \epsilon^2 d\hat{\sigma}_2^{\rm Born} . \tag{10}$$

This decomposition will be useful for writing the soft and virtual corrections. The leading-logarithm (LL) cross section is obtained by convoluting the subprocess cross section with the parton densities and summing over the contributing partons:

$$\sigma^{\rm LL}(pp\to ZZ) = \sum_q \int d\hat{\sigma}^{\rm Born}(q\bar{q}\to ZZ)[G_{q/p}(x_1,M^2)G_{\bar{q}/p}(x_2,M^2) + x_1\leftrightarrow x_2]dx_1dx_2 . \tag{11}$$

B. Virtual Processes

The order-α_s virtual corrections to $q\bar{q}\to ZZ$ come from the interference between the Born graphs of Fig. 1 and the virtual graphs shown in Fig. 2. We have evaluated the interference between these amplitudes in N dimensions using the Feynman parametrization technique. There are two mitigating factors which simplify the $q\bar{q}\to ZZ$ virtual calculation. The first is that the calculation does not contain UV singularities since the graphs in Fig. 2 do not contribute to the renormalization of the strong, electromagnetic, or weak coupling constants. The second is that the self-energy insertions on the external quark lines vanish due to the cancellation of the UV and IR divergences.[16] Basically, what happens is that the UV and IR poles cancel when one does not distinguish between them.

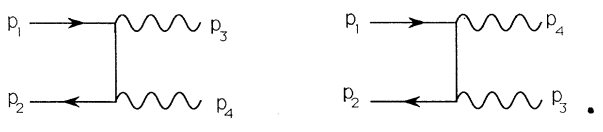

FIG. 1. Feynman diagrams for the Born subprocess $q\bar{q}\to ZZ$. The straight, wavy, and curly lines denote quarks, Z bosons, and gluons, respectively.

Because the loop integrals associated with the four-point function from the box diagrams in Fig. 2 are very difficult to evaluate when powers of the loop momenta appear in the numerator, we first multiply the Born amplitudes times the virtual amplitudes and evaluate the resulting traces. Next, the numerator of the resulting expression is rewritten, using momentum-conservation relations, such that propagator denominator factors cancel with identical factors in the numerator. This way the four-point functions with powers of the loop momentum in the numerator are reduced to a four-point function with a constant numerator and three- and two-point functions which are easier to evaluate. The loop integrals can be reduced to a set of 11 integrals which are given in Appendix B.

The order-α_s virtual contribution to the $q\bar{q}\to ZZ$ cross section is

$$\frac{d\hat{\sigma}^{\rm virt}}{dv} = C_F \frac{\alpha_s}{2\pi} \left(\frac{4\pi\mu^2}{s}\right)^{\epsilon} \frac{\Gamma(1-\epsilon)}{\Gamma(1-2\epsilon)} \left(-\frac{2}{\epsilon^2}\frac{d\hat{\sigma}_0^{\rm Born}}{dv} - \frac{2}{\epsilon}\frac{d\hat{\sigma}_1^{\rm Born}}{dv} - \frac{3}{\epsilon}\frac{d\hat{\sigma}_0^{\rm Born}}{dv} + \frac{1}{4}\frac{1}{9}\frac{1}{2} 4 N_C e^4 [(g_-^{qZq})^4 + (g_+^{qZq})^4][F(t,u) + F(u,t)] \right) , \tag{12}$$

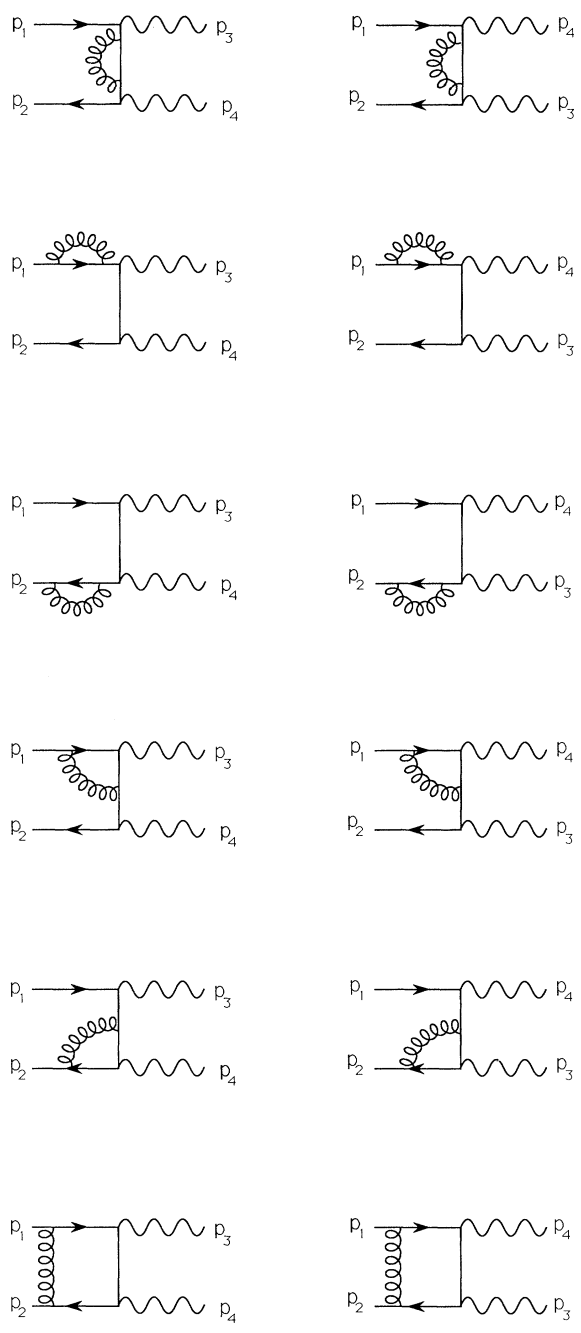

FIG. 2. Feynman diagrams for the virtual subprocess $q\bar{q} \to ZZ$.

where $d\hat{\sigma}_0^{\rm Born}$ and $d\hat{\sigma}_1^{\rm Born}$ are defined by Eq. (10) and $C_F = \frac{4}{3}$ is the quark-gluon vertex color factor. The order-α_s finite corrections are contained in the function $F(t,u)$ which is given in Appendix C. In the limit $M_Z \to 0$, the expression for $d\hat{\sigma}^{\rm virt}(q\bar{q} \to ZZ)$ agrees with the result for $d\hat{\sigma}^{\rm virt}(q\bar{q} \to \gamma\gamma)$ in Ref. 16.

C. Soft-Gluon Emission

The Feynman diagrams for the real emission subprocess

$$q(p_1) + \bar{q}(p_2) \longrightarrow Z(p_3) + Z(p_4) + g(p_5) , \tag{13}$$

are shown in Fig. 3. The soft-gluon amplitude for this subprocess is obtained by setting the gluon momentum p_5 to zero everywhere in the $2 \to 3$ amplitudes except in the denominators which are singular as $p_5 \to 0$. In this approximation the last two graphs in Fig. 3 do not contribute and the $2 \to 3$ kinematics can be approximated by $2 \to 2$ kinematics. The soft-gluon amplitude in $N = 4 - 2\epsilon$ dimensions is

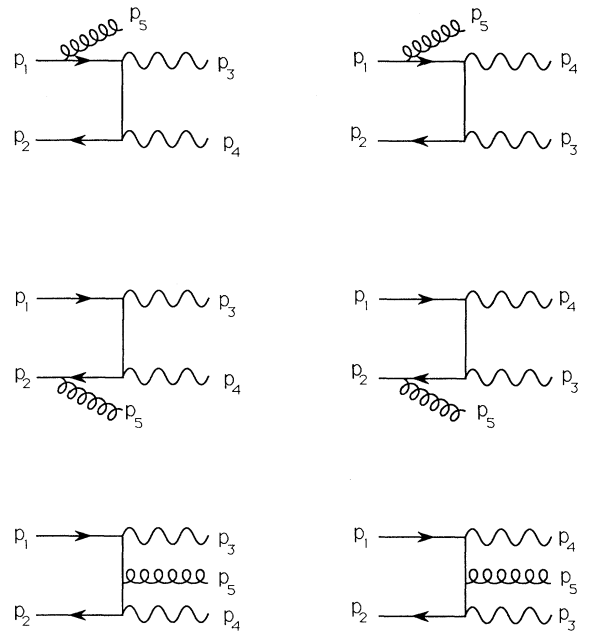

FIG. 3. Feynman diagrams for the real emission subprocess $q\bar{q} \to ZZg$.

$$\mathcal{M}^{\rm soft} = 2\,g_s\,\mu^\epsilon\,T^{i_5}_{i_1 i_2}\,\epsilon^*_\lambda(p_5) \times\left(\frac{p_1^\lambda}{(p_1-p_5)^2}-\frac{p_2^\lambda}{(p_2-p_5)^2}\right)\widetilde{\mathcal{M}}^{\rm Born}\,, \tag{14}$$

where $\widetilde{\mathcal{M}}^{\rm Born}$ is the Born amplitude of Eq. (2) without the $\delta_{i_1 i_2}$ color tensor, g_s is the strong coupling constant, $T^{i_5}_{i_1 i_2}$ is an SU(3) color matrix ($i_1, i_2 = 1,\ldots,3$; $i_5 = 1,\ldots,8$), and $\epsilon^*_\lambda(p_5)$ is the gluon polarization vector. Squaring and summing over final state polarizations and initial state spins yields

$$|\mathcal{M}^{\rm soft}|^2 = 4\,g_s^2\,\mu^{2\epsilon}\,C_F\,\frac{s_{12}}{t_{15}t_{25}}\,|\widetilde{\mathcal{M}}^{\rm Born}|^2\,. \tag{15}$$

Next we introduce a soft-gluon cutoff δ_s and define the soft region of three-body phase space as the region where

$$E_5 < \delta_s\,\frac{\sqrt{s_{12}}}{2}\,. \tag{16}$$

Three-body phase space in N dimensions is given by

$$d^N\Phi_3 = \left(1-\frac{4M_Z^2}{s_{12}}\right)^{1/2-\epsilon}\left(\frac{4\pi^2}{s_{12}}\right)^\epsilon\frac{v^{-\epsilon}(1-v)^{-\epsilon}dv}{2^6\pi^4\Gamma(1-2\epsilon)} \times E_5^{1-2\epsilon}\,dE_5\,\sin^{1-2\epsilon}\theta_1\,\sin^{-2\epsilon}\theta_2\,d\theta_1\,d\theta_2\,, \tag{17}$$

and the soft-gluon contribution to the cross section is given by

$$d\hat\sigma^{\rm soft} = \frac{1}{2s_{12}}\,|\mathcal{M}^{\rm soft}|^2\,d^N\Phi_3\,. \tag{18}$$

Integrating over the soft region of three-body phase space ($0 < E_5 < \delta_s\sqrt{s_{12}}/2$) yields the two-body contribution

$$\frac{d\hat\sigma^{\rm soft}}{dv} = \frac{d\hat\sigma^{\rm Born}}{dv}\,C_F\,\frac{\alpha_s}{2\pi}\left(\frac{4\pi\mu^2}{s}\right)^\epsilon\frac{\Gamma(1-\epsilon)}{\Gamma(1-2\epsilon)} \times\left(\frac{2}{\epsilon^2}-\frac{4}{\epsilon}\ln(\delta_s)+4\,\ln(\delta_s)^2\right)\,. \tag{19}$$

Expanding $d\hat\sigma^{\rm Born}$ as in Eq. (10), this result becomes

$$\frac{d\hat\sigma^{\rm soft}}{dv} = C_F\,\frac{\alpha_s}{2\pi}\left(\frac{4\pi\mu^2}{s}\right)^\epsilon\frac{\Gamma(1-\epsilon)}{\Gamma(1-2\epsilon)}\left[\frac{2}{\epsilon^2}\frac{d\hat\sigma_0^{\rm Born}}{dv}+\frac{2}{\epsilon}\left(-2\,\ln(\delta_s)\frac{d\hat\sigma_0^{\rm Born}}{dv}+\frac{d\hat\sigma_1^{\rm Born}}{dv}\right) +4\,\ln(\delta_s)^2\frac{d\hat\sigma_0^{\rm Born}}{dv}-4\,\ln(\delta_s)\frac{d\hat\sigma_1^{\rm Born}}{dv}+2\frac{d\hat\sigma_2^{\rm Born}}{dv}\right]\,. \tag{20}$$

D. Hard Collinear Corrections

The $2\to3$ real emission processes have hard collinear singularities when $t_{15}\to0$ or $t_{25}\to0$. These singularities must be factorized and absorbed into the initial state parton distributions. The collinear regions of three-body phase space are defined to be those regions where any invariant (s_{ij} or t_{ij}) becomes smaller in magnitude than $\delta_c s_{12}$, where δ_c is the collinear cutoff parameter defined previously. If the collinear cutoff is made sufficiently small, then in the collinear region the three-body process can be evaluated using the leading-pole approximation. In this form it is easy to integrate the logarithmically singular term in N dimensions. The resulting pole in ϵ must then be factorized and absorbed into the appropriate structure function. This procedure is discussed in detail in Ref. 9. After the factorization is performed, the remnants of the hard collinear singularities take the form

$$\frac{d\tilde\sigma}{dv}(q\bar q\to ZZ) = \frac{\alpha_s}{2\pi}\,\frac{d\hat\sigma_0^{\rm Born}}{dv}\left\{G_{q/p}(x_1,M^2)\int_{x_2}^{1-\delta_s}\frac{dz}{z}\left[G_{\bar q/p}\left(\frac{x_2}{z},M^2\right)\tilde P_{qq}(z)+G_{g/p}\left(\frac{x_2}{z},M^2\right)\tilde P_{qg}(z)\right] +G_{\bar q/p}(x_2,M^2)\int_{x_1}^{1-\delta_s}\frac{dz}{z}\left[G_{q/p}\left(\frac{x_1}{z},M^2\right)\tilde P_{qq}(z)+G_{g/p}\left(\frac{x_1}{z},M^2\right)\tilde P_{qg}(z)\right]\right\}, \tag{21}$$

with

$$\tilde P_{ij}(z) \equiv P_{ij}(z)\,\ln\left(\frac{1-z}{z}\,\delta_c\,\frac{s}{M^2}\right)-P'_{ij}(z)-\lambda F_{ij}(z)\,. \tag{22}$$

The Altarelli-Parisi splitting functions in $N = 4-2\epsilon$ dimensions for $0 < z < 1$ are

$$P_{qq}(z,\epsilon) = C_F\left(\frac{1+z^2}{1-z}-\epsilon(1-z)\right)\,,$$
$$P_{qg}(z,\epsilon) = \frac{1}{2(1-\epsilon)}\left[z^2+(1-z)^2-\epsilon\right]\,, \tag{23}$$

and can be written

$$P_{ij}(z,\epsilon) = P_{ij}(z)+\epsilon P'_{ij}(z)\,, \tag{24}$$

which defines the P'_{ij} functions. The functions F_{qq} and F_{qg} depend on the choice of factorization convention and the parameter λ specifies the factorization convention; $\lambda = 0$ for the universal ($\overline{\rm MS}$) convention and $\lambda = 1$ for the physical [deep-inelastic-scattering (DIS)] convention. For the physical convention the factorization functions are

$$F_{qq}(z) = C_F\left[\frac{1+z^2}{1-z}\ln\left(\frac{1-z}{z}\right) - \frac{3}{2}\frac{1}{1-z} + 2z + 3\right],$$

$$F_{qg}(z) = \frac{1}{2}\left[[z^2+(1-z)^2]\ln\left(\frac{1-z}{z}\right) + 8z(1-z) - 1\right]. \tag{25}$$

The parameter M^2 is the factorization scale which must be specified in the process of factorizing the collinear singularity. Basically, it determines how much of the collinear term is absorbed into the various parton distributions.

The upper limit on the integrals appearing in Eq. (21) is determined by requiring that the hard collinear term not overlap with the soft region previously discussed. If such an overlap were to occur, then that region of three-body phase space would be counted twice.

E. Soft Collinear Subtraction Term

The M^2-dependent subtraction piece which is used to absorb the collinear singularity into the parton distribution functions involves an integral over splitting functions with the upper limit corresponding to $z = 1$, not $1 - \delta_s$. Therefore, there is one last piece to be subtracted which, for the t_{15} case, takes the form

$$\frac{d\hat{\sigma}^{15}}{dv} = \frac{d\hat{\sigma}^{\rm Born}}{dv}\frac{\alpha_s}{2\pi}\left(\frac{4\pi\mu^2}{M^2}\right)^{\epsilon}\frac{\Gamma(1-\epsilon)}{\Gamma(1-2\epsilon)} \times \int_{1-\delta_s}^{1}\frac{dz}{z}\left(-\frac{1}{\epsilon}P_{qq}(z) + \lambda F_{qq}(z)\right) G_{q/p}(x/z). \tag{26}$$

In the interval $0 \le z \le 1$ the Altarelli-Parisi splitting function is

$$P_{qq}(z) = C_F\left(\frac{1+z^2}{(1-z)_+} + \frac{3}{2}\delta(1-z)\right) \tag{27}$$

and the factorization-dependent function is

$$F_{qq}(z) = C_F\left[(1+z^2)\left(\frac{\ln(1-z)}{1-z}\right)_+ - \frac{3}{2}\frac{1}{(1-z)_+} - \frac{1+z^2}{1-z}\ln(z) + 2z + 3 - \left(\frac{9}{2} + \frac{\pi^2}{3}\right)\delta(1-z)\right]. \tag{28}$$

The $(\,)_+$ distributions in P_{qq} and F_{qq} are defined in terms of their integrals with an arbitrary function $f(z)$,

$$\int_0^1 f(z)\frac{1}{(1-z)_+}dz \equiv \int_0^1 \frac{f(z)-f(1)}{1-z}dz,$$
$$\int_0^1 f(z)\left(\frac{\ln(1-z)}{1-z}\right)_+ dz \equiv \int_0^1 [f(z)-f(1)]\frac{\ln(1-z)}{1-z}dz. \tag{29}$$

Inserting P_{qq} and F_{qq} into Eq. (26), integrating, and using the expansion

$$\left(\frac{4\pi\mu^2}{M^2}\right)^{\epsilon} = \left(\frac{4\pi\mu^2}{s}\right)^{\epsilon}\left(\frac{s}{M^2}\right)^{\epsilon} = \left(\frac{4\pi\mu^2}{s}\right)^{\epsilon}\left[1 + \epsilon\ln\left(\frac{s}{M^2}\right)\right], \tag{30}$$

yields

$$\frac{d\hat{\sigma}^{15}}{dv} = -C_F\frac{\alpha_s}{2\pi}\left(\frac{4\pi\mu^2}{s}\right)^{\epsilon}\frac{\Gamma(1-\epsilon)}{\Gamma(1-2\epsilon)}\left\{\frac{1}{\epsilon}\left(\frac{3}{2} + 2\ln(\delta_s)\right)\frac{d\hat{\sigma}_0^{\rm Born}}{dv} + \left(\frac{3}{2} + 2\ln(\delta_s)\right)\left[\ln\left(\frac{s}{M^2}\right)\frac{d\hat{\sigma}_0^{\rm Born}}{dv} + \frac{d\hat{\sigma}_1^{\rm Born}}{dv}\right] + \lambda\left(\frac{9}{2} + \frac{\pi^2}{3} + \frac{3}{2}\ln(\delta_s) - \ln(\delta_s)^2\right)\frac{d\hat{\sigma}_0^{\rm Born}}{dv}\right\}. \tag{31}$$

In obtaining this result we have discarded all terms which are proportional to a power of the soft cutoff δ_s. The soft collinear singularity in the $t_{25} \to 0$ region yields an identical result.

F. Next-to-Leading-Logarithm Cross Section

The NLL cross section, which consists of two- and three-body contributions, can now be assembled from the pieces described in the previous sections. The two-body contribution is

$$\sigma_{\rm 2\,body}^{\rm NLL}(pp \to ZZ) = \sum_q \int dv\, dx_1\, dx_2\left(G_{q/p}(x_1, M^2)\, G_{\bar{q}/p}(x_2, M^2)\frac{d\hat{\sigma}^{\rm NLL}}{dv}(q\bar{q} \to ZZ) + (x_1 \leftrightarrow x_2) + \frac{d\tilde{\sigma}}{dv}\right), \tag{32}$$

where the sum is over all contributing quark flavors, $d\tilde{\sigma}/dv$ is defined in Eq. (21), and

$$\frac{d\hat{\sigma}^{\rm NLL}}{dv}(q\bar{q} \to ZZ) = \frac{d\hat{\sigma}^{\rm Born}}{dv} + \frac{d\hat{\sigma}^{\rm virt}}{dv} + \frac{d\hat{\sigma}^{\rm soft}}{dv} - \frac{d\hat{\sigma}^{15}}{dv} - \frac{d\hat{\sigma}^{25}}{dv} . \quad (33)$$

The $1/\epsilon^2$ and $1/\epsilon$ poles cancel when the terms in Eq. (33) are summed [see Eqs. (9), (12), (20), and (26)].

The three-body contribution to the cross section is

$$\sigma_{3\,\rm body}(pp \to ZZ + X) = \sum_{abc} \int d\hat{\sigma}(ab \to ZZc)[\, G_{a/p}(x_1, M^2)\, G_{b/p}(x_2, M^2) + (x_1 \leftrightarrow x_2)]dx_1\, dx_2 , \quad (34)$$

where the sum is over all partons contributing to the three subprocesses $q\bar{q} \to ZZg$, $qg \to ZZq$, and $\bar{q}g \to ZZ\bar{q}$. The squared matrix elements for these subprocesses are given in Appendix D. The integration over three-body phase space and $dx_1\, dx_2$ is done numerically by standard Monte Carlo techniques. The kinematic invariants s_{ij} and t_{ij} are first tested for soft and collinear singularities. If an invariant for a subprocess falls in a soft or collinear region of phase space, the contribution from that subprocess is not included in the cross section.

IV. RESULTS

The numerical results presented in this section have been obtained using the HMRS[18] set B parton distribution functions with $\Lambda_4 = 0.190$ GeV. These distribution functions have been fit at the NLL level using the universal ($\overline{\rm MS}$) convention. Thus the factorization defining parameter λ in Eqs. (22) and (31) should be $\lambda = 0$. [If one instead uses the DFLM[19] parton distribution functions, which are NLL fits defined in the physical (DIS) scheme, then one must set $\lambda = 1$.] A single scale $Q^2 = M_{ZZ}^2$, where M_{ZZ} is the invariant mass of the Z pair, is used for the renormalization and factorization scales. The two-loop expression for α_s has been used and $\Lambda_{\rm QCD}$ adjusted whenever a heavy-quark threshold is crossed so that α_s is a continuous function of Q^2. For the heavy quark masses we use $m_b = 5$ GeV and $m_t = 140$ GeV. The soft and collinear cut-off parameters were taken to be $\delta_s = 5 \times 10^{-2}$ and $\delta_c = 10^{-3}$. We use the standard-model parameters $M_Z = 91.17$ GeV, $M_W = 80.0$ GeV, and $\alpha(M_W) = 1/128$. These mass values are consistent with recent measurements at the Fermilab Tevatron,[20] the SLAC Linear Collider,[21] and the CERN e^+e^- collider LEP.[22] For comparison we also give LL predictions which have been obtained using the two-loop expression for α_s. Using the two-loop running coupling for both the LL and NLL results provides a consistent expansion parameter so that one can judge the degree of convergence of the results.

The $O(\alpha_s)$ corrections to ZZ production have previously been estimated[7] using the soft-gluon approximation.[8] The assumption in this approach is that the π^2 terms are the dominant part of the $O(\alpha_s)$ corrections. Futhermore, the approach assumes that all of the $O(\alpha_s)$ π^2 terms are found by considering only the most singular contributions when the real- or virtual-gluon momentum $k^\mu \to 0$. Thus, the idea is to examine all graphs that give $1/\epsilon^2$ poles and deal with them in the infrared limit. The QCD corrections are thus expressed as a multiplicative K factor times the lowest-order cross section. The soft-gluon K factor derived in Ref. 7 is $K = 1 + \frac{8}{9}\pi\alpha_s$.

The NLL total cross section for Z-pair production is shown in Fig. 4 as a function of the center-of-mass energy. The predicted cross sections for the Tevatron, the CERN Large Hadron Collider (LHC), and the SSC are also given in Table I. Also given are the LL predictions with and without the soft-gluon K factor, $K = 1 + \frac{8}{9}\pi\alpha_s$. Both the NLL and LL plus K-factor results show a significant increase over the pure leading-logarithm calculation. Furthermore, the results indicate that the soft-gluon K-factor estimate is in reasonable agreement with the NLL result for this particular observable. This point will be discussed in more detail below.

One of the motivations for performing NLL calculations is that the results often show a less dramatic dependence on the renormalization and factorization scale choice than the LL result. This is true for the present calculation. As an example, consider first the total cross section at the Tevatron. Here the LL result is nearly in-

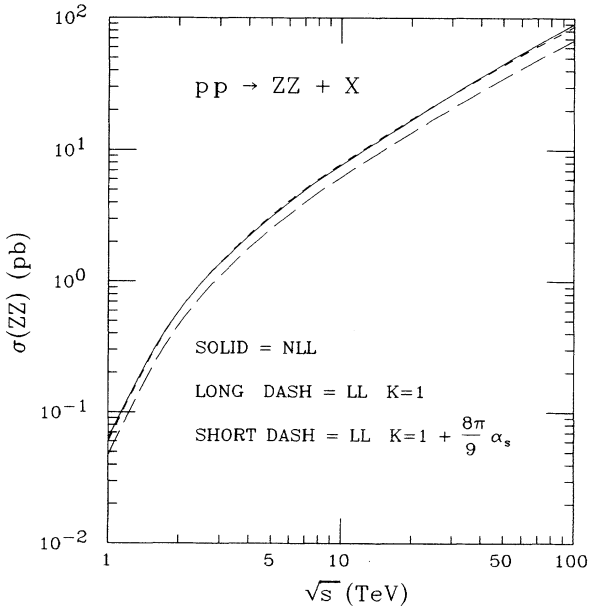

FIG. 4. The total cross section for $pp \to ZZ + X$ as a function of the center-of-mass energy. The solid line is the NLL result, the long-dashed line is the LL result, and the short-dashed line is the LL calculation with a K-factor $K = 1 + \frac{8}{9}\pi\alpha_s$.

TABLE I. Predicted cross sections for ZZ production with no cuts.

Collider	$\sqrt{s}$ (TeV)	$\sigma^{\rm NLL}$ (pb)	$\sigma^{\rm LL}(K=1+\frac{8}{9}\pi\alpha_s)$ (pb)	$\sigma^{\rm LL}(K=1)$ (pb)
Tevatron	1.8	1.08	1.08	0.854
LHC	16	13.3	13.5	10.7
SSC	40	35.6	35.2	28.0

dependent of the scale choice, decreasing only by a factor of 0.94 as Q^2 is varied from $0.5M_{ZZ}^2$ to $2M_{ZZ}^2$. At this energy, ZZ production via $p\bar{p}$ interactions is dominated by valence-quark interactions with x values in a range above a lower limit governed by $M_Z/\sqrt{s}$ which is about 0.05. For these values there is little Q^2 dependence in the valence distributions. On the other hand, at the SSC the relevant x range is smaller by a factor of twenty and sea-quark interactions dominate in the pp process. These distributions show a significant increase with Q^2 in this x region. Over the same range of Q^2 the cross section now increases by a factor of 1.14. When the NLL calculation is examined in a similar way, the cross section at the Tevatron also shows a slight decrease, the factor being 0.96. On the other hand, the cross section at the SSC increases by a factor of 1.03. Hence, there is a lessening of the scale dependence in the NLL results, with the effect being most noticeable at the higher energy of the SSC.

The structure of the NLL calculation given in this paper makes it clear that there is significant cancellation between the positive-definite $2 \rightarrow 3$ contribution and the sum of all the $2 \rightarrow 2$ contributions. Indeed, the latter quantity is not positive definite, as can be seen by examining the results presented in Ref. 9, for example, where the individual cross-section contributions in the case of direct photon production are shown. In the cases where essentially all of the recoil gluon phase space are integrated over, it appears that the cancellation just mentioned is such that the remainder is well approximated by the soft-gluon K factor. However, suppose that one was interested in an observable defined in such a way that the integration over the recoil gluon was severely limited. In this case one might expect to see departures from the soft-gluon K-factor estimate.

Consider, for example, the inclusive transverse-momentum spectrum of the Z bosons, as shown in Fig. 5. The inclusion of the $2 \rightarrow 3$ real emission processes in the NLL calculation shifts events in the distribution from lower to higher values of transverse momentum since the Z pair can now recoil against a gluon. The shape change becomes more pronounced at higher center-of-mass energies as is seen by comparing parts (a) and (b) of Fig. 5 which are for the Tevatron and SSC energies, respectively. Including the K factor in the LL result only scales up the overall normalization and does not predict any shape change.

A similar effect is shown in Fig. 6 for the ZZ invariant-mass distribution. Again, the greater phase space for the recoiling gluon in the higher-energy case results in an increase of the NLL calculation over the approximate one. Consider, however, what would happen if one required that there be no accompanying jet with $p_T(\text{jet}) > 30$ GeV and $|\eta(\text{jet})| < 3$. The results are shown in Fig. 7 and one can see that this restriction has no effect on either the LL or approximate soft-gluon calculations. However, the NLL curve is significantly reduced since a large segment of the positive-definite three-body part has been eliminated by the choice of cuts. The point which we wish to

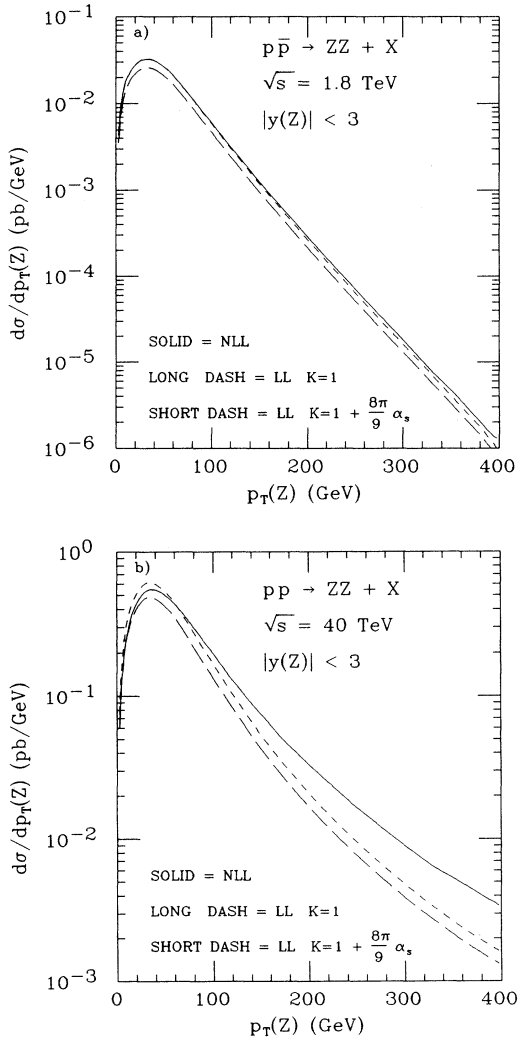

FIG. 5. Inclusive Z-boson transverse-momentum distribution: (a) is for $p\bar{p} \rightarrow ZZ + X$ at $\sqrt{s} = 1.8$ TeV, (b) is for $pp \rightarrow ZZ + X$ at $\sqrt{s} = 40$ TeV. The labeling conventions are the same as Fig. 4.

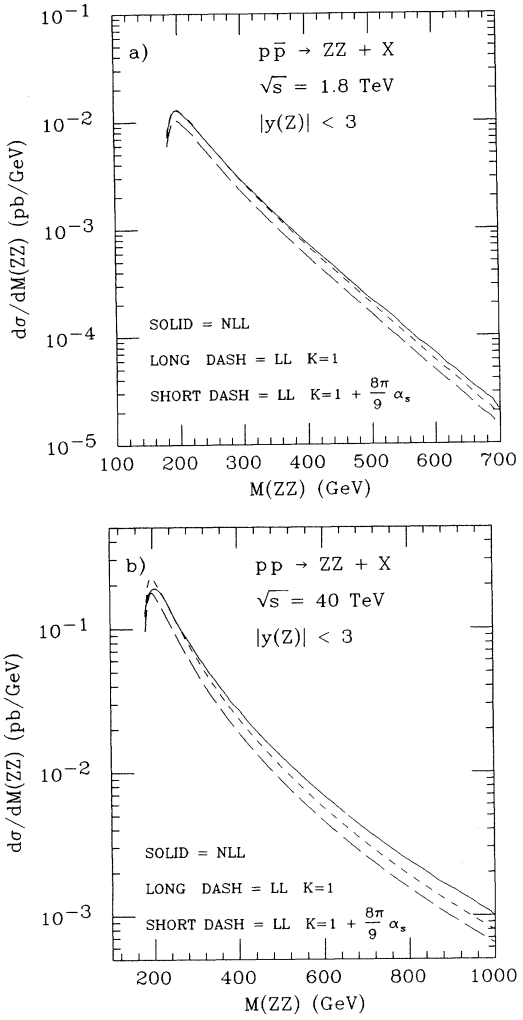

FIG. 6. Invariant-mass distribution for the Z pair. The labeling conventions are the same as Fig. 4.

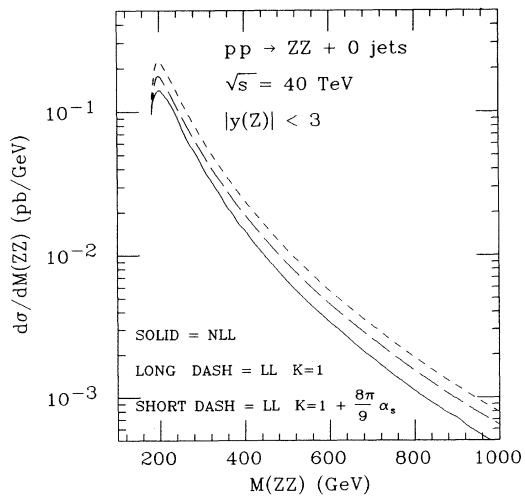

FIG. 7. Same as Fig. 6(b) but no jets are allowed in the final state. The jet criteria are: $p_T(\text{jet}) > 30$ GeV and $|\eta(\text{jet})| < 3$.

emphasize is that the cuts imposed at the analysis stage may be such as to invalidate the use of a simple overall K-factor estimate with the result that the full NLL calculation should be used.

V. SUMMARY

A complete next-to-leading-logarithm calculation of $p\overset{(-)}{p} \to ZZ$ has been presented. The calculation was done using a combination of analytic and Monte Carlo integration methods which make it easy to calculate a variety of observables and to impose experimental cuts. It is interesting to note that for the total ZZ cross section, the NLL corrections were reasonably approximated by including the soft-gluon K factor, $K = 1 + \frac{8}{9}\pi\alpha_s$, in the LL calculation. On the other hand, when typical experimental cuts were imposed, significant differences between the soft-gluon K factor and the full NLL calculation were noted. This is consistent with results obtained previously for direct photon production and jet photoproduction which showed that the size of the NLL corrections depends on the observable being studied. An overall multiplicative K factor is incapable of reproducing this amount of detail.

Note added. After completing this work we learned of a recent order-α_s calculation of the total cross section for hadronic ZZ production by Mele, Nason, and Ridolfi.[26] We have compared results for the total cross section and found them to be in agreement.

ACKNOWLEDGMENTS

We thank H. Baer for useful discussions. This work was supported in part by the U.S. Department of Energy.

APPENDIX A: REGULARIZATION OF γ_5

The implementation of γ_5 in dimensional regularization requires a prescription for defining γ_5. We use the definition proposed by Chanowitz *et al.*,[23] who define γ_5 by the following properties.

(1) $\{\gamma_5, \gamma^\mu\} = 0$, $\mu = 0, 1, \ldots, N-1$.

(2) $\gamma_5^2 = 1$.

(3) $\mathrm{Tr}(\gamma_5\gamma^\mu\gamma^\nu\gamma^\omega\gamma^\tau) = 4i\epsilon^{\mu\nu\omega\tau} + O(N-4) \times$ ambiguity when μ, ν, ω, τ, are in the four-dimensional subspace $\mu, \nu, \omega, \tau = 0, 1, 2, 3$. The Adler-Bell-Jackiw anomaly[24] is related to the fact that the ambiguous term cannot be explicitly defined.

The ambiguous terms are discussed in Ref. 25, where it is shown that they can be discarded. The three defining properties plus the fact that there are not enough vectors to form a nonzero contraction with $\epsilon^{\mu\nu\omega\tau}$ allow one to eliminate traces containing γ_5.

After the ambiguous terms have been discarded and the traces containing γ_5 have been eliminated, we can evaluate the traces in N dimensions using the algebra manipulation program FORM.[15] All γ-matrix algebra was done in N dimensions and the results were checked in four dimensions.

APPENDIX B: LOOP INTEGRALS

The loop integrals from the virtual graphs of Fig. 2 can be reduced to a set of 11 integrals which are given in this appendix. They are written here with a common overall factor

$$F = \left(\frac{4\pi}{s}\right)^{\epsilon} \frac{\Gamma(1-\epsilon)}{\Gamma(1-2\epsilon)} \frac{1}{(4\pi)^2} . \tag{B1}$$

Integrals I_5, I_6, I_7 are infrared and ultraviolet finite and can be evaluated in four dimensions; however, the other integrals are singular and must be regularized. Dimensional regularization was used to regularize these integrals, with the number of space-time dimensions set to $N = 4-2\epsilon$. In all cases the integrals were evaluated using the Feynman parametrization technique. Integrals $I_5^{\mu\nu}$ and I_6^{μ} are only needed for the cases where the indices are contracted with $p_{1\mu}p_{1\nu}$ and $p_{1\mu}$, respectively. The one-point function is defined to be zero in dimensional regularization. The integrals are most conveniently written in terms of functions denoted E_i and B_i. The E_i functions are

$$\begin{aligned}
E_0 &= \left[\ln\left(\frac{-(a_1-b_1)^2}{s}\right) - \ln\left(\frac{-a_1^2}{s}\right)\right] - \frac{\epsilon}{2}\left[\ln\left(\frac{-(a_1-b_1)^2}{s}\right)^2 - \ln\left(\frac{-a_1^2}{s}\right)^2\right] , \\
E_1 &= a_1^2\left[1-\epsilon\ln\left(\frac{-a_1^2}{s}\right)\right] - (a_1-b_1)^2\left[1-\epsilon\ln\left(\frac{-(a_1-b_1)^2}{s}\right)^2\right] , \\
E_2 &= a_1^4\left[1-\epsilon\ln\left(\frac{-a_1^2}{s}\right)\right] - (a_1-b_1)^4\left[1-\epsilon\ln\left(\frac{-(a_1-b_1)^2}{s}\right)^2\right] ,
\end{aligned} \tag{B2}$$

and the B_i functions are

$$\begin{aligned}
B_1(t,u) = {} & \mathrm{Li}_2\left(\frac{M_Z^2-u}{s}\right) - \mathrm{Li}_2\left(\frac{s-M_Z^2}{s}\right) - \mathrm{Li}_2\left(\frac{-st}{(s-M_Z^2)(M_Z^2-t)}\right) + \mathrm{Li}_2\left(\frac{-t}{s-M_Z^2}\right) + \mathrm{Li}_2\left(\frac{M_Z^2}{M_Z^2-t}\right) \\
& -\tfrac{1}{2}\ln\left(\frac{-st}{(s-M_Z^2)(M_Z^2-t)}\right)^2 + \tfrac{1}{2}\ln\left(\frac{-t}{s-M_Z^2}\right)^2 + \tfrac{1}{4}\ln\left(\frac{M_Z^2}{M_Z^2-t}\right)^2 + \tfrac{1}{4}\ln\left(\frac{M_Z^2-t}{s}\right)^2 \\
& -\tfrac{1}{4}\ln\left(\frac{sM_Z^2}{t^2}\right)^2 + \ln\left(\frac{M_Z^2-t}{s}\right)\ln\left(\frac{M_Z^2-u}{-t}\right) - \tfrac{1}{2}\ln\left(\frac{M_Z^2-t}{s}\right)\ln\left(\frac{sM_Z^2}{t^2}\right) , \\
B_7 = {} & \frac{1}{x}\left[-4\,\mathrm{Li}_2\left(\frac{1-x}{2}\right) + 2\ln\left(\frac{1-x}{2}\right)^2 - \ln\left(\frac{s}{M_Z^2}\right)^2 + \frac{\pi^2}{3}\right] ,
\end{aligned} \tag{B3}$$

where $x = \sqrt{1-4M_Z^2/s}$ and $\mathrm{Li}_2(z)$ is the dilogarithm function

$$\mathrm{Li}_2(z) = -\int_0^1 \ln(1-tz)\frac{dt}{t} = \sum_{k=1}^{\infty}\frac{z^k}{k^2} .$$

The eleven integrals are

$$\begin{aligned}
I_1 &\equiv \int \frac{d^Nk}{(2\pi)^N} \frac{1}{k^2(k+p_1)^2(k+p_1-p_3)^2(k-p_2)^2} \\
&= i\frac{F}{st}\left[\frac{1}{\epsilon^2} + \frac{2}{\epsilon}\ln\left(\frac{M_Z^2}{-t}\right) + \frac{2\pi^2}{3} - 2B_1(t,u)\right] ,
\end{aligned}$$

$$\begin{aligned}
I_2^{\mu\nu} &\equiv \int \frac{d^Nk}{(2\pi)^N} \frac{k^\mu k^\nu}{k^2(k+a_1)^2(k+b_1)^2} \\
&= \frac{iF}{4a_1\cdot b_1}\left(-a_1^\mu a_1^\nu E_0 - \frac{a_1^\mu b_1^\nu + b_1^\mu a_1^\nu}{2a_1\cdot b_1}(a_1^2E_0+E_1) + \frac{g^{\mu\nu}}{2}(1/\epsilon+3)E_1\right. \\
&\qquad \left. + \frac{b_1^\mu b_1^\nu}{(2a_1\cdot b_1)^2}[a_1^4(2/\epsilon+3)E_0 + a_1^2(4/\epsilon+10)E_1 - (1/\epsilon+2)E_2]\right) , \quad a_1^2 \neq 0, \quad b_1^2 = 0,
\end{aligned}$$

$$I_3^\mu \equiv \int \frac{d^N k}{(2\pi)^N} \frac{k^\mu}{k^2(k+a_1)^2(k+b_1)^2}$$
$$= \frac{iF}{2a_1\cdot b_1}\left(a_1^\mu E_0 - \frac{b_1^\mu}{2a_1\cdot b_1}[a_1^2(1/\epsilon+1)E_0 + (1/\epsilon+2)E_1]\right), \quad a_1^2 \neq 0, \quad b_1^2 = 0,$$
$$I_4 \equiv \int \frac{d^N k}{(2\pi)^N} \frac{1}{k^2(k+a_1)^2(k+b_1)^2} = \frac{iF}{2a_1\cdot b_1}\frac{E_0}{\epsilon}, \quad a_1^2 \neq 0, \quad b_1^2 = 0,$$

$$p_{1\mu}p_{1\nu}I_5^{\mu\nu} \equiv p_{1\mu}p_{1\nu}\int \frac{d^N k}{(2\pi)^N} \frac{k^\mu k^\nu}{(k+p_1)^2(k+p_1-p_3)^2(k-p_2)^2}$$
$$= i\frac{Fs}{16}\left[2B_7\frac{M_Z^4}{s^2}\left(2\frac{(M_Z^2-t)^2}{M_Z^4} + 4\frac{u-t}{M_Z^2}\frac{M_Z^2-t}{s-4M_Z^2} + 3\frac{(t-u)^2}{(s-4M_Z^2)^2} - \frac{s}{s-4M_Z^2}\right)\right.$$
$$\left. - \ln\left(\frac{s}{M_Z^2}\right)\left(\frac{2M_Z^2-s}{s-4M_Z^2} + \frac{10M_Z^2-s}{s}\frac{(t-u)^2}{(s-4M_Z^2)^2} + 8\frac{u-t}{s}\frac{M_Z^2-t}{s-4M_Z^2}\right) - 1 + \frac{(t-u)^2}{s(s-4M_Z^2)}\right],$$

$$p_{1\mu}I_6^\mu \equiv p_{1\mu}\int \frac{d^N k}{(2\pi)^N} \frac{k^\mu}{(k+p_1)^2(k+p_1-p_3)^2(k-p_2)^2}$$
$$= i\frac{F}{2}\left[B_7\left(\frac{M_Z^2-t}{s} + \frac{M_Z^2}{s}\frac{u-t}{s-4M_Z^2}\right) - \frac{u-t}{s-4M_Z^2}\ln\left(\frac{s}{M_Z^2}\right)\right], \tag{B4}$$

$$I_7 \equiv \int \frac{d^N k}{(2\pi)^N} \frac{1}{(k+p_1)^2(k+p_1-p_3)^2(k-p_2)^2} = i\frac{F}{s}B_7,$$

$$I_8^\mu \equiv \int \frac{d^N k}{(2\pi)^N} \frac{k^\mu}{k^2(k+p_1)^2(k-p_2)^2} = i\frac{F}{s}(p_1^\mu - p_2^\mu)\left(\frac{1}{\epsilon}+2\right),$$

$$I_9 \equiv \int \frac{d^N k}{(2\pi)^N} \frac{1}{k^2(k+p_1)^2(k-p_2)^2} = i\frac{F}{s}\left(\frac{1}{\epsilon^2} - \frac{\pi^2}{3}\right),$$

$$I_{10}^\mu \equiv \int \frac{d^N k}{(2\pi)^N} \frac{k^\mu}{(k+a_1)^2(k+b_1)^2} = -i\frac{F}{2}(a_1^\mu + b_1^\mu)\left[\frac{1}{\epsilon} + 2 - \ln\left(\frac{-(a_1-b_1)^2}{s}\right)\right],$$

$$I_{11} \equiv \int \frac{d^N k}{(2\pi)^N} \frac{1}{(k+a_1)^2(k+b_1)^2} = iF\left[\frac{1}{\epsilon} + 2 - \ln\left(\frac{-(a_1-b_1)^2}{s}\right)\right].$$

APPENDIX C: FINITE VIRTUAL CORRECTIONS

The finite virtual corrections for the subprocess $q\bar{q} \to ZZ$ are contained in the function $F(t,u)$:

$$F(t,u) = A_1(t,u)B_1(t,u) + A_2(t,u)\left[\pi^2 + \ln\left(\frac{s}{-t}\right)^2 - \ln\left(\frac{M_Z^2}{s}\right)^2\right]$$
$$+A_3(t,u)\ln\left(\frac{M_Z^2}{-t}\right) + A_4(t,u)\ln\left(\frac{s}{-t}\right) + A_5(t,u)\ln\left(\frac{M_Z^2}{s}\right) + A_6(t,u)\pi^2 + A_7(t,u)B_7 + A_8(t,u). \tag{C1}$$

The B_i functions are given in Appendix B and the A_i are functions of s, t, u, and M_Z^2:

$$A_1(t,u) = 4 + 4\frac{t}{u} + 2\frac{u}{t} + 16\frac{M_Z^4}{tu} - 8\frac{M_Z^2}{t} - 4\frac{M_Z^4}{t^2} - 16\frac{M_Z^2}{u},$$

$$A_2(t,u) = \frac{t}{M_Z^2-t}\left(-2\frac{t}{u} + 10\frac{M_Z^2}{u} - 2 + \frac{uM_Z^2}{t^2} + 8\frac{M_Z^6}{t^2u} - 2\frac{M_Z^4}{t^2} - 2\frac{M_Z^6}{t^3} - \frac{u}{t} - 16\frac{M_Z^4}{tu} + 6\frac{M_Z^2}{t}\right),$$

$$A_3(t,u) = 4 + 4\frac{t}{u} + 4\frac{u}{t} + 12\frac{M_Z^4}{tu} - 8\frac{M_Z^2}{t} - 8\frac{M_Z^4}{t^2} - 8\frac{M_Z^2}{u}$$
$$+ \frac{t}{M_Z^2-t}\left(3\frac{t}{u} - 5\frac{M_Z^2}{u} + 8 - 4\frac{uM_Z^2}{t^2} - 5\frac{M_Z^6}{t^2u} - 4\frac{M_Z^4}{t^2} + 8\frac{M_Z^6}{t^3} + 10\frac{u}{t} + 7\frac{M_Z^4}{tu} - 18\frac{M_Z^2}{t}\right),$$

$$A_4(t,u) = 6 + 3\frac{t}{u} + 3\frac{u}{t} + 5\frac{M_Z^4}{tu} - 8\frac{M_Z^2}{t} - 3\frac{M_Z^4}{t^2} - 10\frac{M_Z^2}{u} + \frac{t^2}{(M_Z^2-t)^2}\left(-4\frac{t}{u} + 24\frac{M_Z^2}{u} - 4 - 46\frac{M_Z^4}{tu} + 18\frac{M_Z^2}{t} + 2\frac{uM_Z^2}{t^2} + 28\frac{M_Z^6}{t^2u} - 18\frac{M_Z^4}{t^2}\right),$$

$$A_5(t,u) = \frac{t^2}{(M_Z^2-t)^2}\left(4 + 4\frac{u}{t} + 6\frac{M_Z^4}{tu} - 14\frac{M_Z^2}{t} + 4\frac{uM_Z^4}{t^3} + 16\frac{M_Z^8}{t^3u} - 16\frac{M_Z^6}{t^3} - 6\frac{uM_Z^2}{t^2} - 20\frac{M_Z^6}{t^2u} + 22\frac{M_Z^4}{t^2}\right) + 3\frac{t}{u} + \frac{M_Z^4}{tu} - 2\frac{M_Z^2}{t} - 6\frac{M_Z^4}{t^2} + \frac{t}{s-4M_Z^2}\left(-4\frac{M_Z^2}{u} - 1 + \frac{u^2}{t^2} - 2\frac{uM_Z^2}{t^2} + 4\frac{u}{t} + 2\frac{M_Z^2}{t}\right) + \frac{t^2}{(s-4M_Z^2)^2}\left(-\frac{t}{u} - 8\frac{M_Z^2}{u} + \frac{u}{t} + 8\frac{M_Z^2}{t}\right), \tag{C2}$$

$$A_6(t,u) = \frac{1}{3}\left(-6 - 7\frac{t}{u} - 16\frac{M_Z^4}{tu} + 28\frac{M_Z^2}{t} + 4\frac{M_Z^4}{t^2}\right),$$

$$A_7(t,u) = \frac{t^2}{su} - 4\frac{tM_Z^2}{su} - 3\frac{t}{s} + 2\frac{M_Z^4}{st} + 4\frac{M_Z^2}{s} + 4\frac{t}{u} - 8\frac{M_Z^2}{t} + \frac{2M_Z^2}{s-4M_Z^2}\left(\frac{t^2}{su} - 4\frac{tM_Z^2}{su} - \frac{t}{s} + 4\frac{M_Z^2}{s} + \frac{t}{u} + \frac{M_Z^2}{t} - 1\right) + \frac{6M_Z^4}{(s-4M_Z^2)^2}\frac{t}{s}\left(1 - \frac{t}{u}\right),$$

$$A_8(t,u) = \frac{t^2}{(M_Z^2-t)^2}\left(-4\frac{t}{u} + 28\frac{M_Z^2}{u} - 4 - 70\frac{M_Z^4}{tu} + 22\frac{M_Z^2}{t} - 2\frac{uM_Z^4}{t^3} - 28\frac{M_Z^8}{t^3u} + 18\frac{M_Z^6}{t^3} + 2\frac{uM_Z^2}{t^2} + 74\frac{M_Z^6}{t^2u} - 36\frac{M_Z^4}{t^2}\right) + \frac{t}{s-4M_Z^2}\left(1 - \frac{t}{u}\right) + 6 + 3\frac{M_Z^4}{tu} - 6\frac{M_Z^2}{t} + 5\frac{M_Z^4}{t^2} - 8\frac{M_Z^2}{u}.$$

APPENDIX D: REAL EMISSION PROCESSES

The six Feynman diagrams which contribute to the amplitude for the real emission subprocess

$$q(p_1) + \bar{q}(p_2) \longrightarrow Z(p_3) + Z(p_4) + g(p_5) \tag{D1}$$

are shown in Fig. 3. The squared amplitude summed over final state polarizations and initial state spins can be written

$$|\mathcal{M}^{\text{real}}|^2 = 16\,\pi\,\alpha_s\,e^4\,[(g_-^{qZq})^4 + (g_+^{qZq})^4] \sum_{\substack{i=1,6\\ j=i,6}} M_{ij}\,, \tag{D2}$$

where the M_{ij} term corresponds to the squared amplitude from the product of the ith and jth Feynman diagrams in Fig. 3. The M_{ij} are functions of the momenta and the Lorentz scalars $s_{ij} = (p_i + p_j)^2$ and $t_{ij} = (p_i - p_j)^2$:

$$M_{11} = \frac{32p_1\cdot p_5}{t_{15}^2 t_{24}^2}(2p_2\cdot p_4 p_4\cdot p_5 - p_2\cdot p_5 M_Z^2)\,, \quad M_{33} = \frac{32p_2\cdot p_5}{t_{13}^2 t_{25}^2}(2p_1\cdot p_3 p_3\cdot p_5 - p_1\cdot p_5 M_Z^2)\,,$$

$$M_{55} = \frac{16}{t_{13}^2 t_{24}^2}(p_1\cdot p_2 M_Z^4 - 2p_1\cdot p_3 p_2\cdot p_3 M_Z^2 + 4p_1\cdot p_3 p_2\cdot p_4 p_3\cdot p_4 - 2p_1\cdot p_4 p_2\cdot p_4 M_Z^2)\,,$$

$$M_{12} = \frac{128p_1\cdot p_5 p_2\cdot p_5}{t_{15}^2 t_{23} t_{24}}(p_2\cdot p_3 + p_2\cdot p_4 - p_3\cdot p_4)\,,$$

$$M_{13} = \frac{64}{t_{13}t_{15}t_{24}t_{25}}[\,(p_1\cdot p_2)^2(p_3\cdot p_4 - p_3\cdot p_5 - p_4\cdot p_5)$$
$$+p_1\cdot p_2(p_1\cdot p_4 p_3\cdot p_5 + p_1\cdot p_3 p_2\cdot p_5 - p_1\cdot p_4 p_2\cdot p_3 + p_1\cdot p_4 p_2\cdot p_5 - p_1\cdot p_3 p_2\cdot p_4)$$
$$+p_1\cdot p_2(p_1\cdot p_5 p_2\cdot p_3 + p_1\cdot p_5 p_2\cdot p_4 - p_1\cdot p_5 p_3\cdot p_4 + p_2\cdot p_3 p_4\cdot p_5 - p_2\cdot p_5 p_3\cdot p_4)$$
$$+p_1\cdot p_3 p_2\cdot p_5(p_2\cdot p_4 - p_1\cdot p_4) + p_1\cdot p_5 p_2\cdot p_4(p_1\cdot p_3 - p_2\cdot p_3)]\,, \tag{D3}$$

$$M_{14} = \frac{128 p_1\cdot p_2}{t_{14}t_{15}t_{24}t_{25}}(p_1 - p_4)\cdot(p_2 - p_4)(p_1 - p_5)\cdot(p_2 - p_5)\,,$$

$$M_{15} = \frac{64}{t_{13}t_{15}t_{24}^2}[(p_1\cdot p_3 + p_1\cdot p_5 - p_3\cdot p_5)(2p_1\cdot p_4 p_2\cdot p_4 - p_1\cdot p_2 M_Z^2)]\,,$$

$$M_{16} = \frac{64}{t_{14}t_{15}t_{23}t_{24}}\Bigg[(p_1\cdot p_2)^2(p_3\cdot p_5 - p_3\cdot p_4 - p_4\cdot p_5)$$
$$+p_1\cdot p_2(p_1\cdot p_3 p_2\cdot p_4 - p_1\cdot p_3 p_2\cdot p_5 + p_1\cdot p_3 p_4\cdot p_5 + p_1\cdot p_4 p_2\cdot p_3 + p_1\cdot p_4 p_2\cdot p_5)$$
$$+p_1\cdot p_2(p_1\cdot p_5 p_2\cdot p_4 - p_1\cdot p_5 p_2\cdot p_3 - p_1\cdot p_4 p_3\cdot p_5 - p_2\cdot p_4 p_3\cdot p_5 + p_2\cdot p_5 p_3\cdot p_4)$$
$$+p_1\cdot p_5 p_2\cdot p_4(p_2\cdot p_3 - p_1\cdot p_3) + p_1\cdot p_4 p_2\cdot p_3(p_1\cdot p_5 - p_2\cdot p_5) + p_1\cdot p_2 M_Z^2(p_1\cdot p_2 - p_1\cdot p_3 - p_2\cdot p_5)$$
$$+\frac{M_Z^2}{2}(p_1\cdot p_2 p_3\cdot p_5 + p_1\cdot p_3 p_2\cdot p_5 - p_1\cdot p_5 p_2\cdot p_3)\Bigg]\,.$$

The remaining M_{ij} expressions are related to the above expressions by interchanging parton momenta:

$$\begin{aligned}
&M_{22} = M_{11}(p_3 \leftrightarrow p_4), \quad M_{44} = M_{33}(p_3 \leftrightarrow p_4), \quad M_{66} = M_{55}(p_3 \leftrightarrow p_4),\\
&M_{23} = M_{14}(p_3 \leftrightarrow p_4), \quad M_{24} = M_{13}(p_3 \leftrightarrow p_4), \quad M_{25} = M_{16}(p_3 \leftrightarrow p_4),\\
&M_{26} = M_{15}(p_3 \leftrightarrow p_4), \quad M_{34} = M_{12}(p_1 \leftrightarrow p_2),\\
&M_{35} = M_{15}(p_1 \leftrightarrow p_2, p_3 \leftrightarrow p_4), \quad M_{36} = M_{16}(p_1 \leftrightarrow p_2, p_3 \leftrightarrow p_4),\\
&M_{45} = M_{16}(p_1 \leftrightarrow p_2), \quad M_{46} = M_{15}(p_1 \leftrightarrow p_2), \quad M_{56} = M_{14}(p_3 \leftrightarrow p_5).
\end{aligned} \tag{D4}$$

The squared amplitudes for the processes $qg \to ZZq$ and $g\bar{q} \to ZZ\bar{q}$ can be obtained from the $q\bar{q} \to ZZg$ squared amplitude by crossing $p_2 \leftrightarrow -p_5$ and $p_1 \leftrightarrow -p_5$, respectively. Furthermore, one has to correct for an overall minus sign and change the color average from $\frac{1}{3}\times\frac{1}{3}$ to $\frac{1}{3}\times\frac{1}{8}$.

The subprocess cross section in 4 dimensions is

$$d\hat{\sigma}(q\bar{q} \to ZZg) = \frac{1}{4}A_C\frac{1}{2}\frac{1}{2s_{12}}|\mathcal{M}|^2\, d^4\Phi_3\,, \tag{D5}$$

where the factors $\frac{1}{4}, A_C, \frac{1}{2}$ are the spin-average, color-average, and identical-particle factors, respectively.

[1] B. W. Lee, C. Quigg, and H. Thacker, Phys. Rev. D **16**, 1519 (1977).

[2] R. W. Brown and K. O. Mikaelian, Phys. Rev. D **19**, 922 (1979).

[3] J. C. Pumplin, W. W. Repko, and G. L. Kane, in *Proceedings of the Summer Study on the Physics of the Superconducting Super Collider*, Snowmass, Colorado, 1986, edited by R. Donaldson and J. N. Marx (Division of Particles and Fields of the APS, New York, 1986); D. A. Dicus, C. Kao, and W. W. Repko, Phys. Rev. D **36**, 1570 (1987); D. A. Dicus, *ibid.* **38**, 394 (1988).

[4] E. W. N. Glover and J. J. van der Bij, Phys. Lett. B **219**, 488 (1989); Nucl. Phys. **B321**, 561 (1989).

[5] M. J. Duncan, G. L. Kane, and W. W. Repko, Nucl. Phys. **B272**, 517 (1986); M. J. Duncan, Phys. Lett. B **179**, 393 (1986); A. Abbasabadi and W. W. Repko, *ibid.* **199**, 286 (1986); R. Kleiss and W. J. Stirling, *ibid.* **182**, 75 (1986); J. F. Gunion, J. Kalinowski, and A. Tofighi-Niaki, Phys. Rev. Lett. **57**, 2351 (1986); D. A. Dicus, S. L. Wilson, and R. Vega, Phys. Lett. B **192**, 231 (1987); A. Abbasabadi and W. W. Repko, Nucl. Phys. **B292**, 461 (1987); Phys. Rev. D **36**, 289 (1987); **37**, 2668 (1988); D. A. Dicus and R. Vega, *ibid.* **37**, 2474 (1988).

[6] U. Baur, E. W. N. Glover, and J. J. van der Bij, Nucl. Phys. **B318**, 106 (1989); V. Barger, T. Han, J. Ohnemus, and D. Zeppenfeld, Phys. Rev. D **41**, 2782 (1990).

[7] V. Barger, J. L. Lopez, and W. Putikka, Int. J. Mod. Phys. A **3**, 2181 (1988).

[8] A. P. Contogouris, S. Papadopoulos, and J. P. Ralston, Phys. Rev. D **25**, 1280 (1982); A. P. Contogouris

and H. Tanaka, *ibid.* **33**, 1265 (1986); N. Mebarki and H. Tanaka, Mod. Phys. Lett. A **2**, 735 (1987).
[9]H. Baer, J. Ohnemus, and J. F. Owens, Phys. Rev. D **42**, 61 (1990); Phys. Lett. B **234**, 127 (1990).
[10]H. Baer, J. Ohnemus, and J. F. Owens, Phys. Rev. D **40**, 2844 (1989).
[11]L. Bergmann, Ph.D. dissertation, Florida State University, Report No. FSU-HEP-890215.
[12]H. Baer and M. H. Reno, Phys. Rev. D **43**, 2892 (1991).
[13]G. 't Hooft and M. Veltman, Nucl. Phys. **B44**, 189 (1972).
[14]W. A. Bardeen, A. J. Buras, D. W. Duke, and T. Muta, Phys. Rev. D **18**, 3998 (1978).
[15]FORM is a computer program for algebra written by J. A. M. Vermaseren (unpublished).
[16]W. L. Van Neerven, Nucl. Phys. **B268**, 453 (1986).
[17]P. Aurenche, R. Baier, A. Douiri, M. Fontannaz, and D. Schiff, Z. Phys. C **29**, 459 (1985).
[18]P. N. Harriman, A. D. Martin, R. G. Roberts, and W. J. Stirling, Phys. Rev. D **42**, 798 (1990).
[19]M. Diemoz, F. Ferroni, E. Longo, and G. Martinelli, Z. Phys. C **39**, 21 (1988).
[20]Collider Detector at Fermilab Collaboration, F. Abe *et al.*, Phys. Rev. Lett. **63**, 720 (1989).
[21]Mark II Collaboration, G. S. Abrams *et al.*, Phys. Rev. Lett. **63**, 724 (1989).
[22]ALEPH Collaboration, D. Decamp *et al.*, Phys. Lett. B **231**, 519 (1989); **235**, 399 (1990); DELPHI Collaboration, P. Aarnio *et al.*, *ibid.* **231**, 539 (1989); L3 Collaboration, B. Adeva *et al.*, *ibid.* **231**, 509 (1989); OPAL Collaboration, M. Z. Akrawy *et al.*, *ibid.* **231**, 530 (1989).
[23]M. Chanowitz, M. Furman, and I. Hinchliffe, Nucl. Phys. **B159**, 225 (1979).
[24]S. L. Adler, Phys. Rev. **177**, 2426 (1969); J. S. Bell and R. Jackiw, Nuovo Cimento Lett. **4**, 329 (1972).
[25]P. Aurenche and J. Lindfors, Nucl. Phys. **B185**, 274 (1981).
[26]B. Mele, P. Nason, and G. Ridolfi, Report No. CERN-TH 5890/90, 1990 (unpublished).